Available online at www.sciencedirect.com
SCIENCE DIRECT®
Journal of Power Sources 128 (2004) 331–342
JOURNAL OF POWER SOURCES
www.elsevier.com/locate/jpowsour

Novel operation and control of an electric vehicle aluminum/air battery system

Xin Zhang, Shao Hua Yang, Harold Knickle*

Department of Chemical Engineering, University of Rhode Island, Kingston, RI 02881, USA

Received 26 August 2003; accepted 20 September 2003

Abstract

The objective of this paper is to create a method to size battery subsystems for an electric vehicle to optimize battery performance. Optimization of performance includes minimizing corrosion by operating at a constant current density. These subsystems will allow for easy mechanical recharging. A proper choice of battery subsystem will allow for longer battery life, greater range and performance. For longer life, the current density and reaction rate should be nearly constant. The control method requires control of power by controlling electrolyte flow in battery sub modules. As power is increased more sub modules come on line and more electrolyte is needed. Solenoid valves open in a sequence to provide the required power. Corrosion is limited because there is no electrolyte in the modules not being used.

Keywords: Electric vehicle; Aluminum air battery; Sub-batteries; Driving patterns; Control; Power required; Flow rates

1. Introduction

An electric vehicle (EV) can be powered by an aluminum/air battery system. This research work focuses on the Al/air battery system, which is actually a small chemical plant, and its optimization using a novel control method. The Al/air battery has been identified as offering high energy density and having sufficient peak power for an electric vehicle. In addition, the Al/air system offers rapid mechanical recharging, and a range that is compatible with internal combustion engine vehicles [1–3].

The output power of an Al/air battery system should vary with the speed of the electric vehicle. For a single Al/air battery system, the total output power is constant. To allow for operation at or near optimum current, the Al/air battery we designed is made up of several sub-batteries [4]. The purpose of multi sub-batteries is to vary the output power of the battery system. The control system makes the sub-batteries operate at conditions that reduce the corrosion of aluminum and maximizes battery life. The corrosion reactions can be reduced when operating with the current around 200 mA/cm^2 (2 kA/m^2), defined as I_{op} [1,5]. Also corrosion is limited because there is no electrolyte in the modules not being used.

We chose the constant current density of 200 mA/cm2 for analysis in this paper. The value can be determined by examining both the performance and selectivity curves. If additives to the electrolyte are to be used these same curves will help to choose the value of the constant current density. In electric vehicle operation the actual value of the current density will vary somewhat about this value.

The Al/air battery system is operated near I_{op} and the change of the output power is realized by changing the total number of working sub-batteries. We need to regulate and control the electrolyte flow of the Al/air battery system to match the requirement of the sub-systems. Analysis of different driving patterns will yield reference input flow rates for design of the control system.

We can obtain the reference inputs of the flow rate control system through the following:

(1) Define a driving pattern.
(2) From the vehicle speed in the driving pattern, estimate the total power required by the electric vehicle at different times.
(3) Determine the size and quantity of sub-batteries needed for the driving pattern.
(4) Calculate the electrolyte flow rate of the Al/air battery system.
(5) Repeat this process for different driving patterns.
(6) Develop the control method for sequencing the solenoid on/off valves.

* Corresponding author. Tel.: +1-401-874-5984; fax: +1-401-782-1066.
E-mail address: knickle@egr.uri.edu (H. Knickle).

0378-7753/$ – see front matter © 2003 Elsevier B.V. All rights reserved.
doi:10.1016/j.jpowsour.2003.09.058

Nomenclature

a	acceleration of the vehicle (km/(h s))
A	the frontal cross-sectional area of the vehicle (m^2)
C_a	dimensionless tire friction coefficient
C_t	dimensionless aerodynamic coefficient
d	air density (kg/m^3)
g	gravitational acceleration (m/s^2)
I_{op}	operating current density of the sub-batteries (mA/cm^2 or kA/m^2)
KE	kinetic energy (kJ)
M	vehicle mass (kg)
P_{accel}	power for acceleration (kW)
P_{aero}	power required by air drag (kW)
$P_{average}$	average power required by the vehicle for given driving pattern (kW)
$P_{inertial}$	inertial losses of rotating components (kW)
P_{grade}	power required for the gradient (kW)
$P_{traction}$	power required for the driving wheel (kW)
P_{tyres}	rolling resistance power consumed by tires (kW)
PE	potential energy of the vehicle (kJ)
Range	range of the vehicle (km)
t	time (min or s)
T	running time of the vehicle (h)
v	vehicle speed (km/h)
$v_{average}$	average speed of the vehicle (nominal) (km/h)
V	volume of the battery (l)

Greek letters

θ	angle of grade
ε	battery to wheel efficiency

2. Modelling equations for power and energy calculations

In order to obtain the reference input of the electrolyte flow rate control system, it is mandatory to quantitatively estimate the power and energy required for propelling a modern car. Neglecting relatively minor losses due to road camber and curvature, the power required at the drive wheel ($P_{traction}$) consists of five major losses. The traction equation may be expressed as [6],

$$P_{traction} = P_{grade} + P_{accel} + P_{tires} + P_{aero} + P_{inertial}, \quad (1)$$

where P_{grade} is the power required for the gradient, P_{accel} the power required for acceleration, P_{tires} the rolling resistance power consumed by the tires, P_{aero} the power consumed by the aerodynamic drag and $P_{inertial}$ includes inertial losses of rotating components.

The first term in Eq. (1) describe the rates of change of potential energy (PE) during climbing. The second term represents the change in kinetic energy or the acceleration component. The power required for these actions may be estimated from Newtonian kinematics as follows.

$$P_{grade} = \frac{d(PE)}{dt} = Mgv\sin\theta \quad (2)$$

and

$$P_{accel} = \frac{d(KE)}{dt} = d\left(\frac{(1/2)Mv^2}{dt}\right) = Mav \quad (3)$$

where M is the mass of the car, v its velocity, a its acceleration, and $\tan\theta$ is the gradient of the road.

The next two terms in Eq. (1) describe the power required to overcome tire friction and aerodynamic drag that are irreversibly lost, mainly as heat and noise and cannot be recovered. The power for these two terms may be estimated from the following empirical relations.

$$P_{tires} = C_t Mgv \quad (4)$$

and

$$P_{aero} = 0.5dC_aA(v+w)^2v \quad (5)$$

where C_t and C_a are dimensionless tire friction and aerodynamic drag coefficients, respectively, d the air density, w the head-wind velocity, g the gravitational acceleration, and A is the frontal cross-sectional area of the car. The last term of $P_{traction}$, which is $P_{inertial}$, is assumed to be a constant of 1 kW in this calculation.

From the parameters associated with a typical modern medium-size car, we have $M = 1400$ kg, $A = 2.2\,m^2$, $C_t = 0.01$, $C_a = 0.3$ and $d = 1.17\,kg/m^3$ [6], and its power requirements may be estimated from Eqs. (2) to (5). The wind speed (w) is taken to be zero for the sake of simplicity.

Fig. 1 represents our calculation of traction power ($P_{traction} - P_{inertial}$) versus car velocity for an electric vehicle at various accelerations and zero gradients.

The linearity of this variable makes the electric vehicle relatively easy to control as speed varies under zero gradient conditions. Figs. 2 and 3 are recalculations of Fig. 1 using gradients of 5° and 10°. These curves also show linearity and thus indicate straightforward control schemes can be used to vary power.

The power of the battery:

$$P = \frac{P_{traction}}{\varepsilon} + P_{other}, \quad (6)$$

where ε is the battery to wheel efficiency, and ε is taken as 0.9. P_{other} is the additional power required to power accessories. In our calculations, we assume there are no accessories, and $P_{other} = 0$. This can be included in an analysis later. It does not affect the driving pattern or traction power.

For a given driving pattern, the average power will be

$$P_{average} = \frac{\int_0^T P\,dt}{T}, \quad (7)$$

where T is the duration of a given driving cycle.

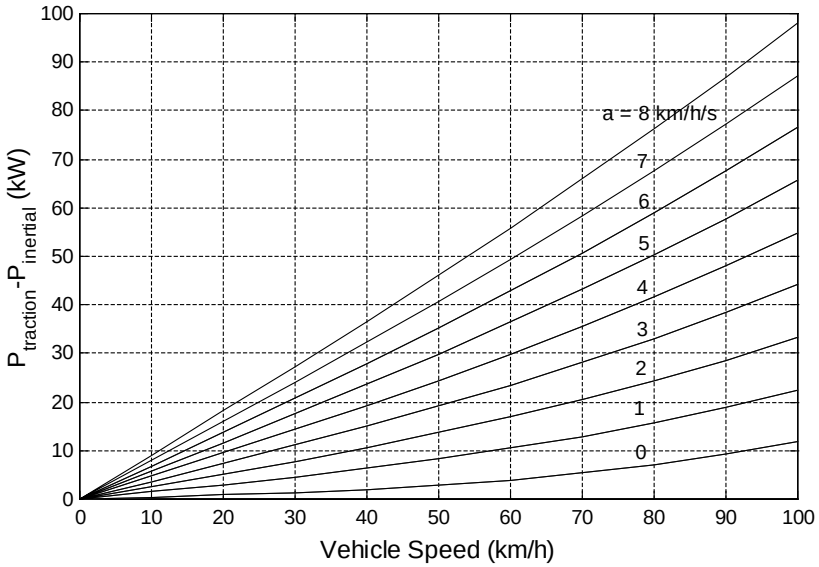

Fig. 1. Power of traction vs. car speed for an electric car at various accelerations and zero degree gradients.

The total energy required by the car is

$$E_{\text{total}} = P_{\text{average}} \times T. \tag{8}$$

The average speed of the car is

$$v_{\text{average}} = \frac{\int_0^T v\,\mathrm{d}t}{T}. \tag{9}$$

The range of the car for a given amount of Al fuel is

$$\text{Range} = v_{\text{average}} \times T \tag{10}$$

While the nominal operating range for replacement of aluminum is about 1600 km and the replacement of electrolyte/water will be required about 400 km (four stops) the actual range will depend upon the driving patterns. In the actual case sensors will warn the driver for both of these conditions. Assuming a battery system carries 80 kg Al, the average energy density in the operation range of interest is about 4 kWh/kg_Al [1]. The total energy is 320 kWh.

3. Aluminum/air battery system

The power system of the electric vehicle consists of four major blocks illustrated in Fig. 4. These four blocks are Al/air battery system, power electric control system, electric motor and vehicle wheels. This research work focuses on the first part, i.e. Al/air battery system, actually a small chemical plant.

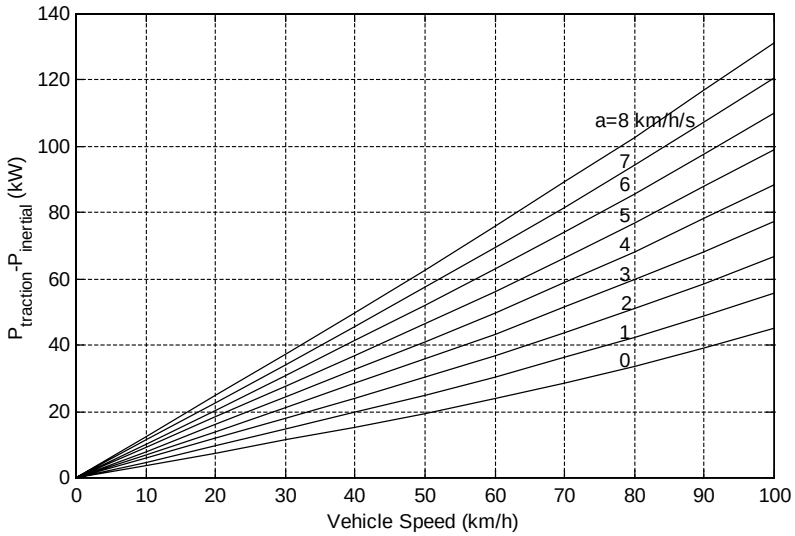

Fig. 2. Power of traction vs. car speed for an electric car at various accelerations and 5° gradient.

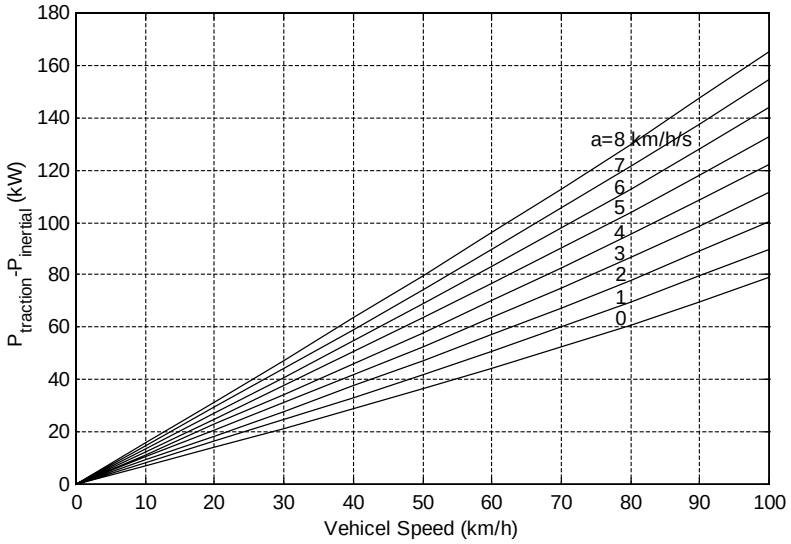

Fig. 3. Power of traction vs. car speed for an electric car at various accelerations and 10° gradient.

The Al/air system has been identified as offering high energy density and having sufficient peak power. In addition, the Al/air system offers rapid mechanical rechargeability, and a range that is compatible with internal combustion engine vehicles [7–11].

An Al/air battery system requires the integration of a number of subunits. These include a battery stack, crystallizer (precipitator), CO_2 absorber, gas separator, cooling system including heat exchanger and components to circulate electrolyte and air and to perform various control functions. Fig. 5 shows a basic interconnection and flow diagram of an Al/air battery system [3]. The reactions in the battery stack generate power. The crystallizer unit controls the electrolyte composition by inducing the soluble reaction product to precipitate on seed crystals contained within the crystallizer. The precipitation process produces the final reaction product and regenerates the electrolyte. The air flow system supplies pressurized air to the cathode where a portion of the oxygen in the air is consumed as one of the battery reactants. The air is first filtered to remove the small amount of CO_2 present. Removing the CO_2 is expected to prolong the life of the air cathode catalyst. The electrolyte that flows out of the battery stack will pass the gas separator for hydrogen separation. Thermal control of the battery is accomplished at the battery stack by the coolant recycling system.

4. Driving patterns

Reference inputs for the electrolyte flow rate control system can be obtained from data or models representing driving patterns. Once we get data for the driving patterns, we can use it to calculate the time dependent power required for the electric vehicle propulsion. We can then determine on average how many sub-batteries should work, the size of the sub-batteries, and finally calculate the electrolyte flow rate of the Al/air battery system and its control.

Figs. 6–9 are four different driving patterns, which represent possible highway driving, urban driving, hybrid driving—local and highway driving, and local driving. These were arbitrarily chosen. There are many other possibilities.

A 44-min cycle is illustrated in Fig. 6. This 44-min cycle is composed of two acceleration segments, i.e. oa and bc, and two braking segments, i.e. de and fg. In segment oa the average speed is 24 km/h and acceleration is 0.8 km/(h s); in segment ab the speed is 48 km/h and no acceleration; in segment bc the average speed is 72 km/h and acceleration is 0.8 km/(h s); in segment cd the speed is 96 km/h and no acceleration; in segment de, ef and fg the average speed is 72, 48 and 24 km/h, respectively. And there is no acceleration in these three segments.

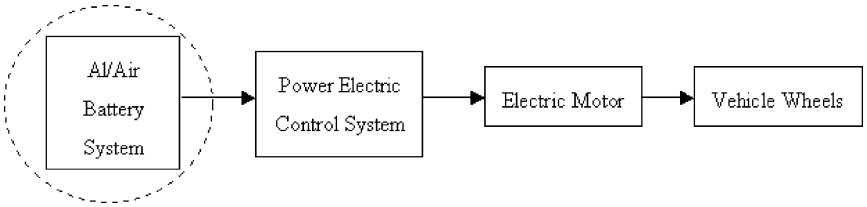

Fig. 4. Power system of an electric vehicle.

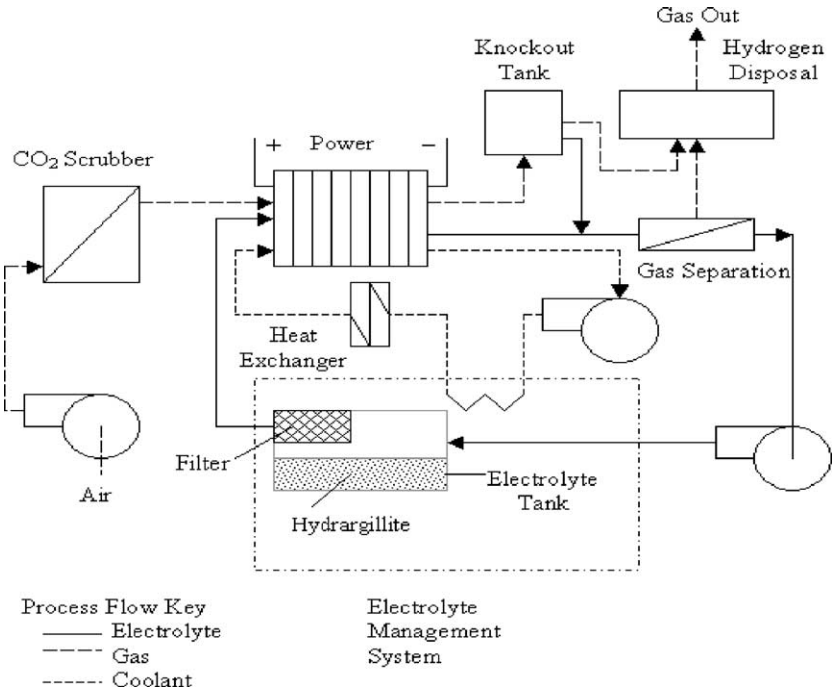

Fig. 5. Basic flow diagram of an Al/air battery system by Gibbons et al. [3].

A 6-min cycle is illustrated in Fig. 7. This 6-min cycle is composed of six 1-min cycles, which contain three 10 s accelerations, two 12 s accelerations, and one 15 s acceleration. All braking segments are 5 s, and rests are 15 s.

In segment oa, hi and uv, the average speed is 20 km/h and acceleration is 4 km/(h s); in segment ab, ij and vw, the speed is 40 km/h and no acceleration; in segment bc, jk and wx, the average speed is 20 km/h and no acceleration; in segment cd, gh, kl, pq, tu and xy, there is a 15 s rest, which speed is zero; in segment de, the average speed is 35 km/h and acceleration is 5.83 km/(h s); in segment ef, the speed is 70 km/h and no acceleration; in segment fg, the average speed is 35 km/h and no acceleration; in segment lm, the average speed is 45 km/h and acceleration is 6 km/(h s); in segment mn, the speed is 90 km/h and no acceleration; in segment np, the speed is 45 km/h and no acceleration; in segment qr the average speed is 27.5 km/h and acceleration is 4.58 km/(h s); in segment rs, the speed is 55 km/h and no acceleration; In segment st, the average speed is 27.5 km/h and no acceleration.

A 7.5-min cycle is shown in Fig. 8. This 7.5-min cycle is composed of a 5-s, three 10-s and two 15-s acceleration; four 5-s, two 10-s and one 15-s braking. All the rests are 5 s. These are constant speed segments ab, ef, gh, ij, kl, mn, pq,

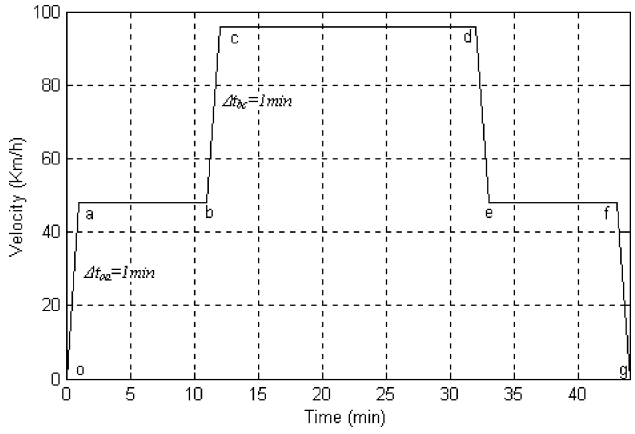

Fig. 6. Example driving pattern 1—highway driving—representing the simplest pattern going to work with total duration of 44 min. *Note*: Δt is the duration of acceleration, which is the same in Figs. 7–9.

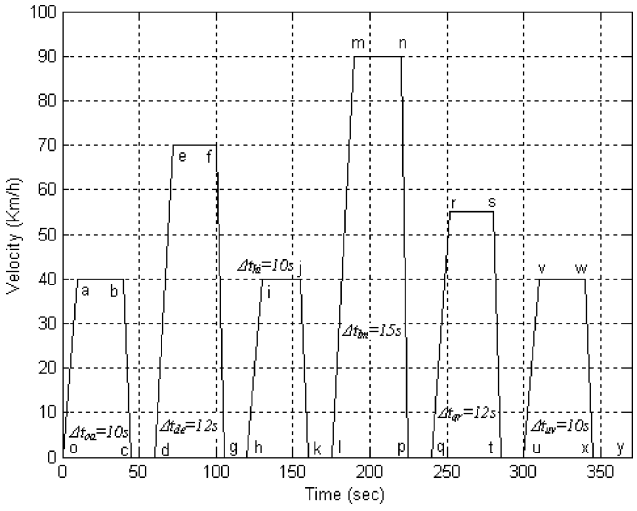

Fig. 7. Example driving pattern 2—urban driving—representing the simplified federal urban driving cycle (SFUDS) with total duration of 6 min [7].

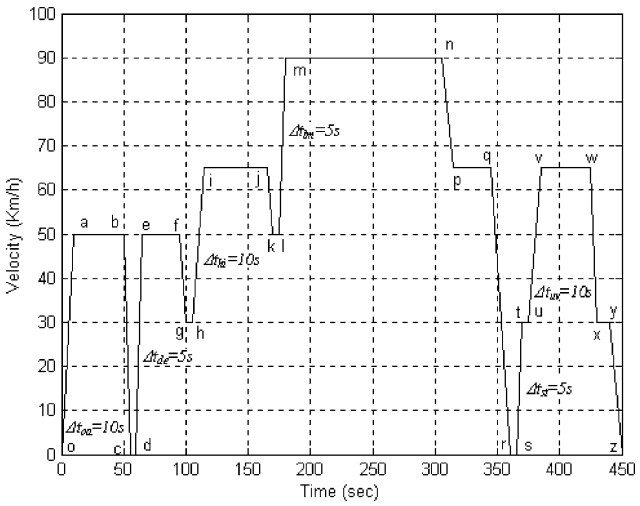

Fig. 8. Example driving pattern 3—hybrid driving—local and highway driving with total duration of 7.5 min.

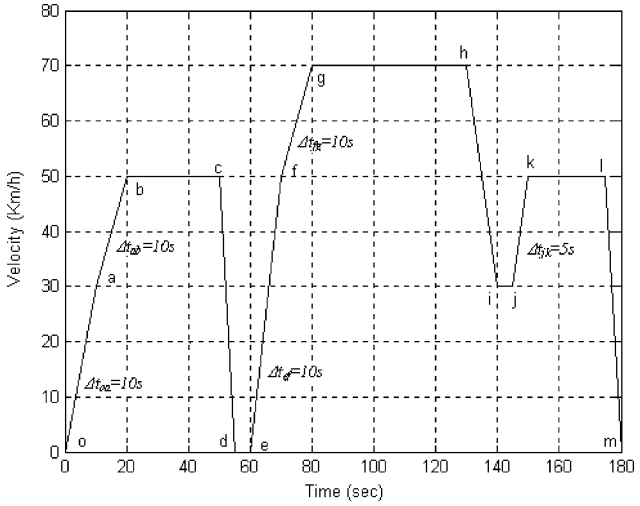

Fig. 9. Example driving pattern 4—local driving—representing shopping driving with total duration of 3 min.

tu, vw and xy, with speeds of 50, 50, 30, 65, 50, 90, 65, 30, 65, 30 km/h, respectively. In acceleration segment oa, de, hi, lm, st and uv, the average speed is 25, 25, 47.5, 70, 15 and 47.5 km/h, respectively. The corresponding accelerations are 5, 10, 3.5, 8, 6 and 3.5 km/(h s), respectively. In braking segment bc, fg, jk, np, qr, wx and yz, the average speed is 25, 40, 57.5, 77.5, 32.5, 47.5 and 15 km/h, respectively, and no acceleration.

A 3-min cycle is illustrated in Fig. 9. This 3-min cycle is composed of a 5-s and four 10-s acceleration; two 5-s and one 10-s braking and one 5-s rest. These constant speed segments bc, gh, ij and kl, are 50, 70, 30 and 50 km/h, respectively. The corresponding acceleration segment oa, ab, ef, fg and jk, have average speeds of 15, 40, 25, 60 and 40 km/h, respectively. The corresponding accelerations are 3, 2, 5, 2 and 4 km/(h s), respectively. In braking segment cd, hi, the average speeds are 25 and 50 km/h, respectively. There is no acceleration for these segments.

5. Power for each driving pattern

Table 1 are calculations of the individual and total requirements making up the traction power. These are calculated from Eqs. (2)–(5). The total power, or traction power is then plotted in Fig. 10.

The above procedure is repeated for the driving patterns of 2, 3, and 4. Traction power calculations are then presented in Tables 2–4, and in Figs. 11–13 accordingly.

The SAE gave a dynamic capacity test on SAE J1798 issued January 1997 [12]. This test is intended to measure the capacity of a battery module under dynamic discharge conditions similar to those which are imposed on electric vehicles in urban driving conditions. This dynamic cycle is scaled to a percentage of the rated or specified maximum power for the module to be tested. We assumed the maximum power for the module to be tested is 50 kW and we used the modified SAE dynamic capacity test profile as one of our power patterns because the Al/air battery system is not charged during driving. The resulting power profile is shown in Fig. 14.

6. Proposed battery system

The proposed battery system total output power is fixed and determined by its structure. When driving an electric

Table 1
Estimated power for an electric car corresponding to driving pattern shown in Fig. 6

Segment	Duration	Velocity	Acceleration	P_{tires}	P_{aero}	P_{grade}	P_{accel}	$P_{inertial}$	$P_{traction}$
oa	1	24	0.8	0.9144	0.1144	0	2.0736	1	4.1024
ab	10	48	0	1.8288	0.9152	0	0	1	3.744
bc	1	72	0.8	2.7432	3.0888	13.716	6.2208	1	26.7688
cd	20	96	0	3.6576	7.3216	0	0	1	11.9792
de	1	72	0	2.7432	3.0888	0	0	1	6.832
ef	10	48	0	1.8288	0.9152	0	0	1	3.7444
fg	1	24	0	0.9144	0.1144	0	0	1	2.0288

Units: duration, min; velocity, km/h; acceleration, km/(h s); power, kW, which is the same in Tables 2–4 except for duration, s.

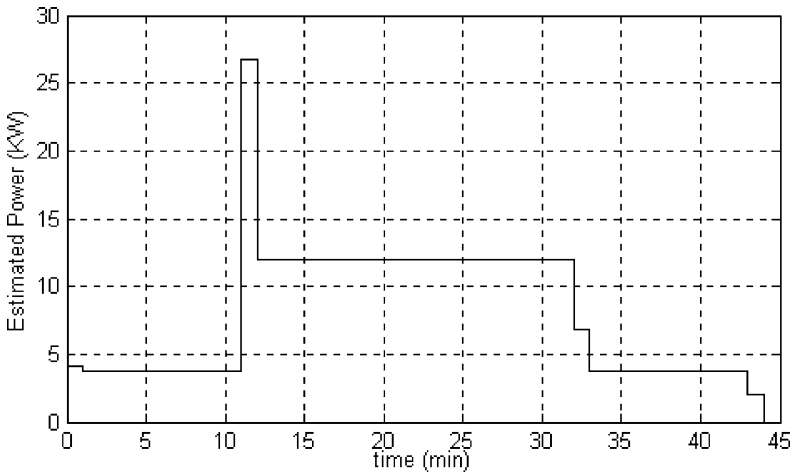

Fig. 10. Estimated power for an electric car corresponding to driving pattern shown in Fig. 6.

car, we need to change vehicle speed to match driving conditions. Thus, it is necessary to regulate the output power of the battery system. A novel structure of the battery stack is proposed in this research to provide the required output power.

The purpose of sub-batteries is to regulate the output power of the Al/air battery system and prolong the lifetime of the whole battery system by making the sub-batteries work in shifts. Each sub-battery is comprised of a number of cells that are responsible for a certain percent of the whole battery power. The electrolyte flow rate in each sub-battery and thus the current density of a single cell in a sub battery is kept at a constant value to reduce the effect of polarization and corrosion. The output power of a single sub-battery is maintained relatively constant. The output power of the whole battery system is proportional to the number of the working sub-batteries. If the power demand of an EV is increased, e.g. in the process of acceleration, more sub-batteries are working. The electrolyte flow rate of the whole battery should be varied in proportion to the number of working sub-batteries. Solenoid valves provide the electrolyte flow to the appropriate number of sub-batteries. If the output power of the battery system increases, the electrolyte flow rate of the whole system should also be increased

Table 2
Estimated power for an electric car corresponding to the driving pattern shown in Fig. 7

Segment	Duration	Velocity	Acceleration	P_{tires}	P_{aero}	P_{grade}	P_{accel}	$P_{inertial}$	$P_{traction}$
oa	10	20	4	0.762	0.0662	0	8.64	1	10.468
ab	30	40	0	1.524	0.5297	0	0	1	3.054
bc	5	20	0	0.762	0.0662	0	0	1	1.828
cd	15	0	0	0	0	0	0	0	0
de	12	35	5.83	1.33	0.3548	6.6675	22.037	1	31.3893
ef	28	70	0	2.667	2.84	0	0	1	6.507
fg	5	35	0	1.33	0.3548	0	0	1	2.685
gh	15	0	0	0	0	0	0	0	0
hi	10	20	4	0.762	0.0662	0	8.64	1	10.468
ij	15	40	0	1.524	0.5297	0	0	1	3.054
jk	5	20	0	0.762	0.0662	0	0	1	1.828
kl	15	0	0	0	0	0	0	0	0
lm	15	45	6	1.71	0.754	17.145	29.16	1	41.1965
mn	30	90	0	3.43	6.03	0	0	1	10.46
np	5	45	0	1.71	0.754	0	0	1	3.464
pq	15	0	0	0	0	0	0	0	0
qr	12	27.5	4.58	1.048	0.172	0	13.6	1	15.82
rs	28	55	0	2.096	1.377	0	0	1	4.473
st	5	27.5	0	1.048	0.172	0	0	1	2.22
tu	15	0	0	0	0	0	0	0	0
uv	10	20	4	0.762	0.0662	0	8.64	1	10.468
vw	30	40	0	1.524	0.5297	0	0	1	3.054
wx	5	20	0	0.762	0.0662	0	0	1	1.828
xy	15	0	0	0	0	0	0	0	0

Table 3
Estimated power for an electric car corresponding to the driving pattern shown in Fig. 8

Segment	Duration	Velocity	Acceleration	P_{tires}	P_{aero}	P_{grade}	P_{accel}	$P_{inertial}$	$P_{traction}$
oa	10	25	5	0.9525	0.1293	0	13.5	1	15.58
ab	40	50	0	1.905	1.034	0	0	1	3.939
bc	5	25	0	0.9525	0.1293	0	0	1	2.082
cd	5	0	0	0	0	0	0	0	0
de	5	25	10	0.9525	0.1293	4.7625	27	1	33.8443
ef	30	50	0	1.905	1.034	9.525	0	1	13.465
fg	5	0	0	1.524	0.5296	0	0	1	3.05
gh	5	30	0	1.143	0.2234	0	0	1	2.366
hi	10	47.5	3.5	1.81	0.887	9.05	17.95	1	30.7
ij	50	65	0	2.476	2.273	0	0	1	5.749
jk	5	57.5	0	2.19	1.573	0	0	1	4.763
kl	5	50	0	1.905	1.034	0	0	1	3.939
lm	5	70	8	2.667	2.838	13.335	60.48	1	80.32
mn	125	90	0	3.429	6.033	0	0	1	10.462
np	10	77.5	0	2.953	3.852	0	0	1	7.805
pq	30	65	0	2.476	2.273	0	0	1	5.749
qr	15	32.5	0	1.24	0.284	0	0	1	2.524
rs	5	0	0	0	0	0	0	0	0
st	5	15	6	0.572	0.0279	0	9.72	1	11.32
tu	5	30	0	1.143	0.223	0	0	1	2.366
uv	10	47.5	3.5	1.81	0.887	0	17.95	1	21.65
vw	40	65	0	2.476	2.273	0	0	1	5.749
wx	5	47.5	0	1.81	0.887	0	0	1	3.697
xy	10	30	0	1.143	0.223	0	0	1	2.366
yz	10	15	0	0.572	0.0279	0	0	1	1.6

proportionally keeping the electrolyte flow rate within a single cell at a constant value. Thus, the regulation of the output power of the Al/air battery system turns into flow rate control problem and control of a set of solenoid valves. During the use of the sub-batteries the unused sub-batteries are empty of electrolyte markedly reducing corrosion in the system.

The concept of sub-batteries for use in an EV is a break-through concept. It not only makes it possible for the output power of the Al/air battery system to vary with different demands, but optimizes use of aluminum and minimizes corrosion. Determining how to size the sub-batteries is a practical problem for the whole battery system design. Driving patterns give the basis for sizing these sub-batteries. Different driving patterns including modified SAE dynamic capacity test profiles [12] are considered in this sub-battery sizing problem.

As shown in Fig. 15, the proposed battery structure for the electric vehicle consists of several sub-batteries that are in parallel to form the whole battery.

The improvement of sub-battery sizing and optimal operation and implementation of this Al/air battery system with hardware requires additional research and design work. It may be possible that the size of all sub-systems are the same. The advantage of this concept includes standardization and easy mechanical recharging.

Table 4
Estimated power for an electric car corresponding to the driving pattern shown in Fig. 9

Segment	Duration	Velocity	Acceleration	P_{tires}	P_{aero}	P_{grade}	P_{accel}	$P_{inertial}$	$P_{traction}$
oa	10	15	3	0.5715	0.0279	0	4.86	1	6.4594
ab	10	40	2	1.524	0.5296	0	8.64	1	11.6936
bc	30	50	0	1.905	1.034	9.525	0	1	13.464
cd	5	25	0	0.9525	0.1293	0	0	1	2.0818
de	5	0	0	0	0	0	0	0	0
ef	10	25	5	0.9525	0.1293	0	13.5	1	15.5818
fg	10	60	2	2.286	1.787	11.43	12.96	1	29.463
gh	50	70	0	2.667	2.838	0	0	1	6.505
hi	10	50	0	1.905	1.034	0	0	1	3.939
ij	5	30	0	1.143	0.223	0	0	1	2.336
jk	5	40	4	1.524	0.5296	0	17.28	1	20.3336
kl	25	50	0	1.905	1.034	0	0	1	3.939
lm	5	25	0	0.9525	0.1293	0	0	1	2.0818

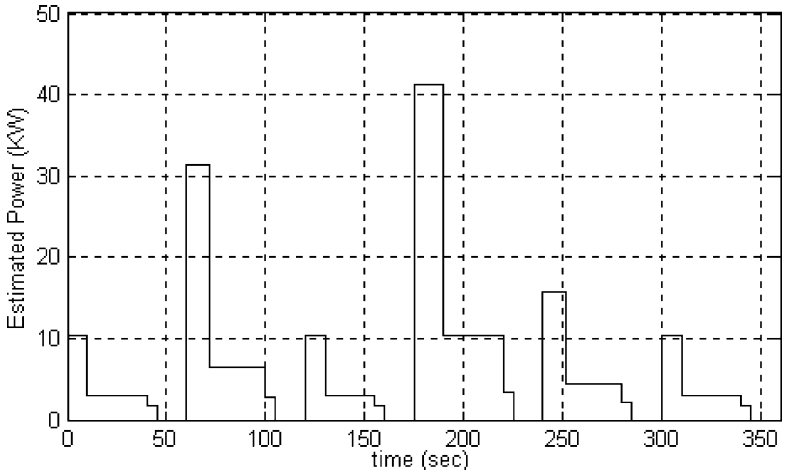

Fig. 11. Estimated power for an electric car corresponding to the driving pattern shown in Fig. 7.

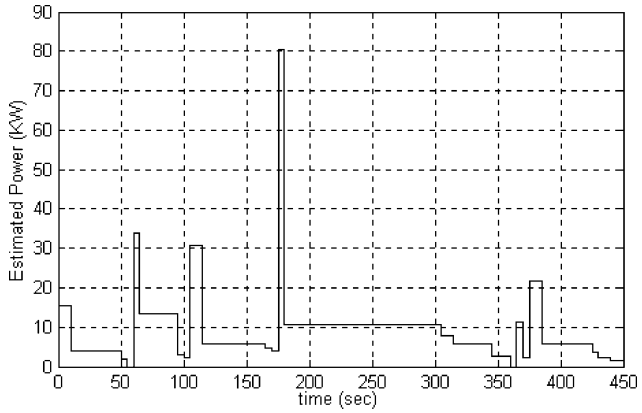

Fig. 12. Estimated power for an electric car corresponding to the driving pattern shown in Fig. 8.

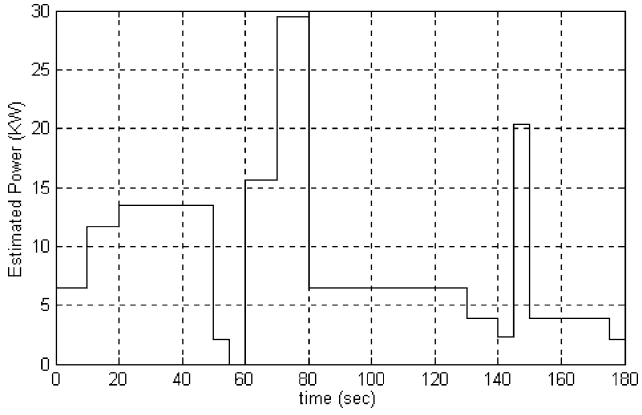

Fig. 13. Estimated power for an electric car corresponding to the driving pattern shown in Fig. 9.

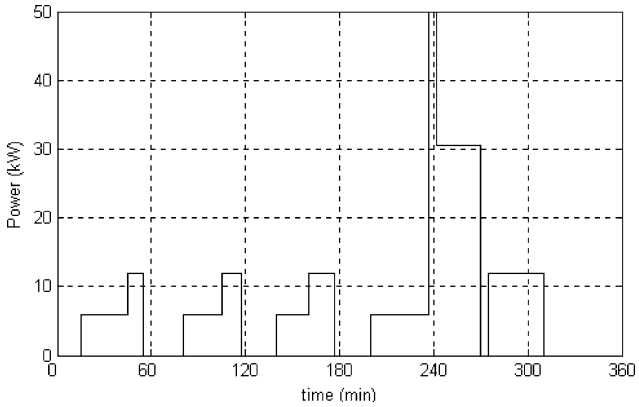

Fig. 14. Modified SAE dynamic capacity test profile [12].

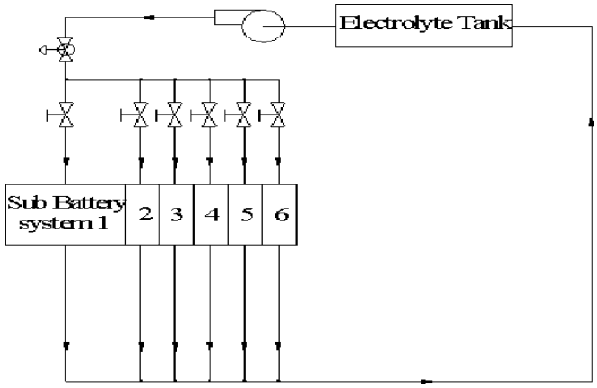

Fig. 15. Electrolyte flow system with on/off valves and battery sub-systems [4].

7. Sizing the modules

As we have discussed in detail before, the whole Al/air battery system is composed of several sub-batteries that will work in shifts. Before obtaining the reference input of the flow rate control system, we need to size the sub-batteries, i.e. determine the output power of each sub-battery. The process to determine the output power of each sub-battery is called battery sizing.

An example structure of an electrolyte flow system for an Al/air battery is shown in Fig. 16. The electrolyte flow

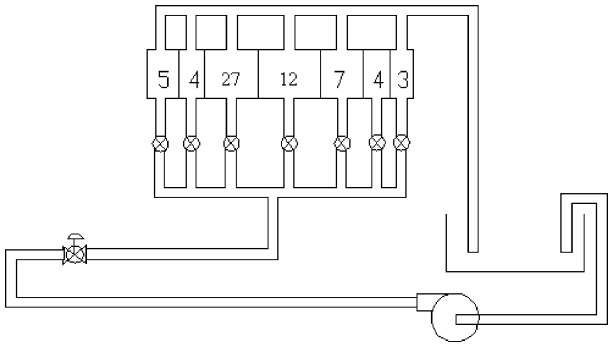

Fig. 16. The electrolyte flow system with sized sub-batteries in kW. Solenoid on/off valves are also indicated.

system of this Al/air battery is comprised of five primary parts, which includes seven sub-batteries, seven solenoid on/off valves, a controllable valve that can be modeled as a first-order system with a small amount of time delay, and an electrolyte tank and a pump. These parts are connected by pipes with a diameter of 4 cm. Each sub-battery is made up of several cells with fixed output voltage. The number of the total cells in a sub-battery is determined by the output power of this sub-battery. All of the cells in the sub-batteries are operated at a constant current, which is I_{op}. The solenoid on/off valves determine the state of the sub-batteries. Since there are only two states of on/off valves, i.e. on or off, the state of the sub-batteries is either working or rest. When the solenoid valve is on, the cells in the corresponding sub-battery are working. When the solenoid valve turns off, there is no electrochemical reaction in the cells. The electrolyte drains into the electrolyte tank.

The simplest way to size the sub-batteries is to make the number of sub-batteries equal to the number of segments on the driving pattern and make the output power of sub-batteries equal to the required $P_{traction}$ in different segments on driving pattern. Here, we use the driving pattern shown in Fig. 6 as an example of this sizing method. In Fig. 6, there are seven segments, so we choose the number of sub-batteries as seven. The output power of each of these seven sub-batteries is equal to the $P_{traction}$ in the different segments, which means the required $P_{traction}$ in segment oa is 4.1024 kW and thus we set the first sub-battery output power to 5 kW. For the second sub-battery we set its output power to 4 kW due to the $P_{traction}$ in segment ab is 3.744 kW. With the same approach, the output powers of sub-battery 3–7 are set to 27, 12, 7, 4 and 3 kW, respectively. However, sizing the sub-batteries with this method may lead to redundant sub-batteries. In this case, there are two sub-batteries whose output power are exactly the same, which is 4 kW. In the mean time, it is clear that sub-batteries with the output power of 7 and 12 kW are also redundant because we can use the sub-batteries with the output power of 3 and 4 kW as a substitution of the one with power of 7 kW, and the combination of the sub-batteries with power of 3, 4 and 5 kW as the sub-battery with power of 12 kW. Hence, another sizing method is necessary to reduce the redundancy of the sub-batteries.

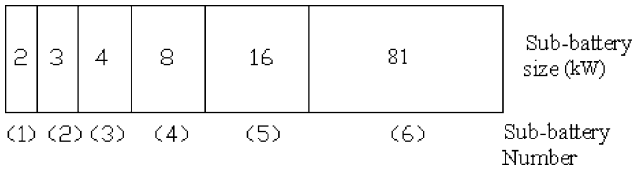

Fig. 17. Structure of sized sub-batteries corresponding to driving pattern shown in Fig. 8.

A more complicated driving pattern is shown in Fig. 8, there are total 25 segments in this driving pattern. In this case, choosing the number of the sub-batteries as the total number of segments in driving pattern is not a practical method. If the number of sub-batteries exceeds more than ten, it will bring some other problems such as increase of complication of the control system, more solenoid valves needed. Generally, the number of sub-batteries is around 7. How to determine the output power of each sub-battery is a critical problem in design. The demanding output power of each segment on driving pattern. Fig. 8 is shown in the column of $P_{traction}$ in Table 3. There are three big numbers in $P_{traction}$, which are 33.8443, 30.7 and 80.32. We can size a part of the sub-batteries with these big numbers in $P_{traction}$. In this case, the output power of one sub-battery can be set to 81 kW, which can provide the $P_{traction}$ of 80.32 kW in segment lm. We use another five sub-batteries in designing this Al/air battery. The output powers of these five sub-batteries are sized at 2, 3, 4, 8 and 16 kW, respectively. These five sub-batteries and combination of some or all of them can provide the demanded $P_{traction}$ in any segment shown in Fig. 8. The structure of these sized sub-batteries is illustrated in Fig. 17.

With the same method we can size the sub-batteries corresponding to other driving patterns in Fig. 7. Fig. 18 gives the sizing result corresponding to driving patterns in Fig. 7.

In the mean time we size the sub-batteries corresponding to the SAE dynamic capacity test profile illustrated in Fig. 14, which is demonstrated in Fig. 19.

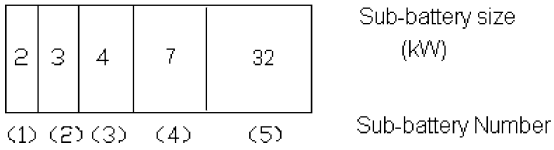

Fig. 18. Structure of sized sub-batteries corresponding to driving pattern shown in Fig. 7.

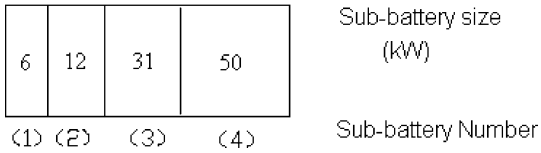

Fig. 19. Structure of sized sub-batteries corresponding to modified SAE dynamic capacity test profile in Fig. 14.

Table 5
Example of an operation sequence of the sub-batteries for driving pattern 1

Segments	Power (kW)	Sub-batteries
oa	5	1
ab	4	2
bc	27	1–3
cd	12	4
de	7	2 and 7
ef	4	6
fg	3	7

8. Battery sub-system operation optimization

The use of sub-batteries in designing the Al/air battery system is to change the output power of the whole battery system and also make it operate in optimum condition to maximize the battery life. When the sub-battery is working, the corresponding solenoid valve is on, the electrolyte flows into the sub-battery. Some corrosion reactions in that sub-battery will take place concurrently with the desired electrochemical reactions. These corrosion reactions will reduce the lifetime of the sub-batteries. Hence, the control system we propose for the Al/air battery system makes the sub-batteries work in shifts to prolong the battery life.

Consider an example of the sub-batteries shown in Fig. 17. We have seven sub-batteries with the output power of 2, 3, 4, 8, 16 and 80 kW, respectively. These seven sub-batteries are numbered from 1 to 6 as shown in Fig. 15. In segment oa, the demanded output power ($P_{traction}$) of Al/air battery is 16 kW, during this time, only sub-battery 5 is working while all the others are in the rest. In segment ab, the $P_{traction}$ is 4 kW, sub-battery 3 is now in a working state and the others rest. In segment ef the power is 23 kW, while no sub-battery has a output power of 23 kW. To achieve 23 kW we use three sub-batteries numbered as 2, 3 and 5 work together.

An operation sequence of the sub-batteries shown in Fig. 16 (driving pattern 1 in Fig. 6) is shown in Table 5.

9. Electrolyte flow rates

A typical flow rate pattern, illustrated in Fig. 20, is obtained from the driving pattern 3 shown in Fig. 8 and is used as the reference input of the flow rate control system. Various control methods and simulations can now be considered to optimize control of the EV.

10. Example of a 100 horsepower electric vehicles system

For a 100 horsepower (75 kW) electric vehicle, we calculated the battery mass and volume. We also calculate the driving range and running time of the vehicle for a given amount of aluminum fuel of 80 kg.

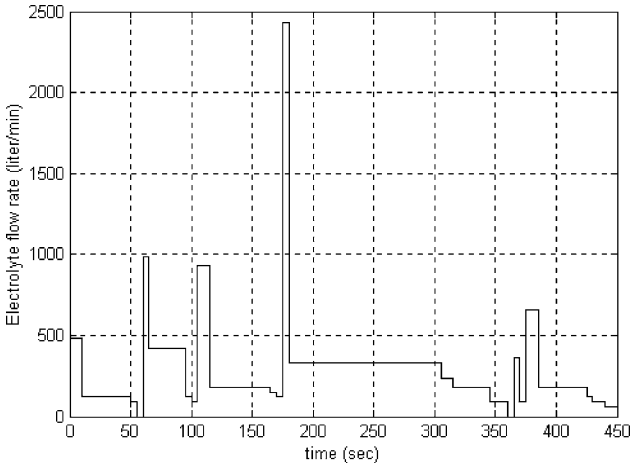

Fig. 20. Example flow rate pattern of aluminum/air battery system corresponding to the driving pattern 3 shown in Fig. 8.

The nominal power is determined by driving patterns summarized in Table 6. The calculation methods for battery mass and volume are the same as in our previous paper [1]. Sample calculations for range and running time are given in Section 10.1. A summary of these results is listed in Table 7.

10.1. Sample driving pattern 1: highway driving

- Battery design characteristics.
- Battery peak power = 75 kW, average battery power = 8.9 kW.
- Peak current density = 5 kA/m^2; peak power density = 6 kW/m^2.
- Sub-battery operating current density = 2 kA/m^2; operating power density = 2.9 kW/m^2.
- Battery weight = 489 kg.
- Battery volume = 679 l.
- Average speed = 70 km/h.
- Anode mass = 80 kg aluminum.
- Anode energy density = 4 kWh/kg_Al.
- Aluminum change: run time T (h) = (anode mass × anode energy density)/ nominal power = (80 × 4)/8.9 = 36.
- Range = average speed × T = 70 × 36 h = 2520 km.
- Electrolyte/water change: four stops, every 9 h, and 630 km to add water.

Table 6
Power requirements and average velocities for different driving patterns

Driving patterns	Peak power (kW)	Average traction power (kW)	Nominal (average) battery power	Average velocity (km/h)
1	75	8	8.9	70
2	75	7	7.8	35
3	75	9	10	61
4	75	9	10	49
Modified SAE test	75	11	12.2	

Table 7
Estimated running time and ranges of the vehicle for different driving patterns

Driving patterns	Peak power (kW)	Normal power (kW)	Average velocity (km/h)	Running time (h)	Range (km)
1	75	8.9	70	36	2520
2	75	7.8	35	41	1435
3	75	10	61	32	1952
4	75	10	49	32	1568
Modified SAE test	75	12.2	–		

Notes: (1) Battery mass 489 kg, anode mass = 80 kg; (2) one stop for change of sub-batteries for the given range; (3) four stops for change of electrolyte for the given range.

The calculation procedures are the same for other driving patterns. The results are shown in Table 7. The results clearly show that the range and running time of the vehicle depends on different driving patterns.

11. Conclusions

This research work focuses on the Al/air battery system and its optimization using a novel control method. The Al/air system also offers rapid mechanical recharging, and a range that is compatible with internal combustion engine vehicles To allow for operation at or near optimum current, the Al/air battery system we propose is made up of several sub-batteries. The purpose of multi sub-batteries is to vary the output power of the battery system. The control system makes the sub-batteries operate at conditions that reduce the corrosion of aluminum and maximize the battery life. Analysis of different driving patterns will yield reference input flow rates for the design of the control system. The linearity of traction power makes the electric vehicle relatively easy to control as speed varies. Reference inputs of the electrolyte flow rate control system are obtained from the data representing driving patterns. Calculations of the individual and total power requirements are included. One or several sub-batteries will work in shifts. Sub-batteries not being used will be void of the electrolyte. After the power of each sub-battery is determined the required flow rates are calculated. Flow rates are used to determine the control system. The use of sub-batteries is a break-through that not only makes the output power of the Al/air battery system vary with demand, but gives a possible way for optimal use of aluminum and minimal corrosion.

For a 100 horsepower (75 kW) electric vehicle, we calculated a battery mass of 489 kg and battery volume of 679 l. The driving range and running time for this example is about 1600 km and the replacement of the electrolyte will be required after about 400 km (four stops). The actual range will depend upon the driving patterns.

The improvement of sub-battery sizing and optimal operation and implementation of this Al/air battery system with hardware will require additional research and design work.

References

[1] S. Yang, H. Knickle, Design and analysis aluminum/air battery system for electric vehicles, J. Power Sources 112 (1) (2002) 162–173.
[2] S. Yang, H. Knickle, Two dimensional transport modeling of an aluminum/air cell, in: Proceedings of the 202nd Meeting of the Electrochemical Society, 2 Nov 2002.
[3] S. Gibbons, W. Daniel, Eric J. Rudd, Development of aluminum/air batteries for propulsion applications, in: Proceedings of the Intersociety Energy Conversion Engineering Conference; Proceedings of the 28th Intersociety Energy Conversion Engineering Conference, vol. 1, 8–13 Aug 1993, Atlanta.
[4] X. Zhang, H. Knickle, Analysis and design of a novel control method for aluminum/air battery system, in: Proceedings of 204th Meeting of the Electrochemical Society, Orlando, Florida, 12–17 October 2003.
[5] S. Yang, H. Knickle, Modeling the performance of an aluminum/air cell, J. Power Sources, in press.
[6] A.K. Shukla, A.S. Aricò, V. Antonucci, An appraisal of electric automobile power sources, Renew. Sustain. Energy Rev. 5 (2001) 137–155.
[7] J.F. Cooper, R.V. Homsy, J.H. Landrun, The Aluminum/air battery for electric vehicles propulsion, in: Proceedings Fifteenth Intersociety Energy Conversion Engineering Conference, Seattle, WA, 18–22 August 1980.
[8] J.F. Cooper, E. Behrin, The Aluminum/Air Battery for Electric Vehicles: An Update, Energy and Technology Review, Lawrence Livermore National Laboratory, Livermore, CA, November 1980.
[9] J.F. Cooper, R.V. Homsy, Development of the Aluminum/Air Battery for Electric Vehicle Applications, Lawrence Livermore National Laboratory, Livermore, CA, UCRL-86560, August 1981.
[10] E. Behrin, Progress Report on the Aluminum/Air Battery, Electronics Engineer, Department Quarterly Report, Lawrence Livermore National Laboratory, Livermore, CA, UCRL-50025-82-1, April 1982.
[11] E. Behrin, R.L. Wood, J.D. Salisbury, D.J. Whisler, C.L. Hudson, Design Analysis of an Aluminum/Air Battery for Vehicle Operations, Lawrence Livermore National Laboratory, Livermore, CA, UCRL-53382, March 1983.
[12] SAE, Surface Vehicle Recommended Practice, SAE J1798, 1997–2001.